Slope Movement Detection Sensor Based on Acceleration Using Multi-Point Fixed Inclinometer

Jestin Jelani[1, a)] Aina Syahirah Ahmad Ishak[1, b)] Zuliziana Suif[1, c)] Nordila Ahmad[1, d)] Ahmad Loqman Ahmad Mazuki[2, e)] Latifah Sarah Supian[2, f)]

[1]*Department of Civil Engineering, Faculty of Engineering, National Defence University of Malaysia, 57000Kuala Lumpur, Malaysia*
[2]*Department of Electric and Electrical Engineering, Faculty of Engineering, National Defence University of Malaysia, 57000Kuala Lumpur, Malaysia*

Corresponding author: [a)] jestin@upnm.edu.my
[b)] ainaishak989@gmail.com
[c)] zuliziana@upnm.edu.my
[d)] nordila@upnm.edu.my
[e)] loqman@upnm.edu.my
[f)] sarah@upnm.edu.my

Abstract. A slope movement detection sensor is a proactive measure to monitor slope failure or landslide. Slope instability significantly contributes to hazards affecting lives and properties. Numerous instruments have been developed to monitor slope movement at the surface or deeper ground. In this study, the application of a slope movement detection sensor, namely the Multi-Point Fixed Inclinometer (MPFI), was illustrated to detect slope movement below the ground surface. The MPFI employs the MPU-9250, a Micro-Electromechanical Systems (MEMS) sensor controlled by an Arduino Mega model 2560 RE, which can detect the precursor movement of the slope prior to failure. The sensor components are enclosed with segmented casing and connected via a flexible wire. Owing to its flexibility, the connection exhibits unrestricted slope movement in all axis directions, rendering it more sensitive compared to a rigid Poly Vinyl Chloride (PVC), metal pipe or concrete encasement. Two units of prototype sensors were assessed on a small-scale slope model made of silica sand with a slope angle of 34°. The slope model is subjected to incremental surcharge load to induce slope failure, and the readings of slope movement are captured by the MPFI. Failure data depicts changes in acceleration behavior from stable to instantaneous spike when there is minute slope movement. The landslide threshold values for the triggering state were interpreted from a series of laboratory experiments when the z, x and y acceleration values were 0.1, 0.1 and 0.01 m/s^2, respectively. The MPFI will be further developed for long-term monitoring with the application of the Internet-of-Thing (IoT) and early warning system.

INTRODUCTION

Landslides or slope failure are prevalent natural geological hazards (geohazard) frequently occurring worldwide. This event is characterized as the movement of a mass of rock, soil or debris down a slope under the influence of gravity [1]. Notably, the stability of a natural slope is influenced by two factors: internal and external factors. The internal factors contribute to the soil's properties, as well as hydrogeological and stress conditions. Meanwhile, the external triggering factors include excessive surcharge load, rainfall, groundwater flow, changes in groundwater level, seepage, steep slope profile, anthropogenic factors, seismicity, and earthquakes, to name a few. Most landslide incidents rarely occur from a single factor. Instead, they develop from several triggering factors that amplify shear stress within the soil mass, exceeding the soil's shear strength [2].

Landslide events in Malaysia have caused a considerable number of fatalities alongside substantial economic and environmental losses after floods. Between 1973 and 2007, around US$ 5 billion was lost due to landslides [3]. The increase in landslide events was attributed to development in high terrain areas, which has caused disturbance to the natural slope. Building on this, the condition is aggravated since Malaysia receives high annual rainfall, with an

average of 2,400 mm [4]. An example of a major landslide that occurred in Malaysia is at Bukit Antarabangsa in 2008, which killed five residents and destroyed 14 bungalows [5]. In another recent incident in 2022, 31 people were killed due to a landslide at Batang Kali, Selangor [6]. These incidents have caused socio-economic impact and social pressure on families, land border conflicts, and soil degradation. Hence, developing slope monitoring and early warning systems is crucial as a preventive measure against landslides to reduce casualties and property losses.

A slope monitoring system has been used to assess the instability of cut slopes since 1960. In particular, it collects and analyzes various data types to determine slope performance and condition. The effectiveness of a slope monitoring system is measured by its ability to issue alerts prior to landslides. Previous studies have employed various data to monitor and quantify landslide threshold value and provide early warning. Furthermore, previous studies have also used rainfall parameters such as rainfall intensity and rainfall duration as threshold values in predicting slope failure based on established empirical rainfall thresholds from past landslide disasters [7,8]. Meanwhile, [9,10] utilized soil-water conditions, i.e. pore water pressure, moisture content, and groundwater level in slope instability evaluation. However, this method can be highly challenging in predicting landslide occurrence due to the difficulty in determining model constant and boundary conditions. Therefore, soil-water condition solely cannot be utilized as a direct indicator to evaluate the instability of a slope [11].

On the other hand, slope deformation or movement is more useful and practical for landslide prediction. Measurement of slope deformation or movement is directly associated with the real movement of the slope. Many methods based on the measurement of slope deformation or movement have been proposed to predict the onset of landslides. Some include the utilization of surface and deep monitoring instrumentations such as extensometer, tilt meter, Global Positioning System (GPS), Differential Interferometric Synthetic Aperture Radar (DInSAR) and total station [12–14].

In this study, underground or deep slope movement detection sensors were developed using 9-axis sensors comprised of an accelerometer, gyroscope, and magnetometer. The basic principle of the Multi-Point Fixed Inclinometer (MPFI) sensor is based on angular rotation, tilt, orientation (with respect to the earth's magnetic north), and velocity of failure mass. The MPFI is designed to be flexible as it does not require rigid PVC pipes or concrete or steel casing. This method allows free movement, thus resulting in accurate slope movement detection prior to landslides. In addition, it is also capable of illustrating the slope movement in 3D. This study aims to develop a prototype of a slope monitoring sensor to detect precursor movement prior to a landslide and determine its threshold value. Accordingly, the prototype sensor is expected to improve disaster risk management by providing early warning alerts and minimizing the impact of landslides on human life and property.

METHODOLOGY

The methodology of this study is divided into two sections. The first part is the development of the prototype MPFI sensor. Lastly, the sensor will be installed and assessed on a small-scale silica sand slope model to detect slope movement and determine the threshold value in terms of acceleration.

Laboratory and Experimental Works

Development of the MPFI sensors

The MPFI sensor is developed using MPU-9250, which has three sensors, and each is equipped with a three-axis configuration: gyroscope, accelerometer, and magnetometer (refer to Fig. 1(a)). The integration of 9-axis motion tracking with an on-board Digital Motion Processor (DMP) enables the sensors to operate as an Initial Measurement Unit (IMU). The sensor operates via I2C connectivity, facilitating comprehensive 9-axis Motion Fusion. The sensor device is then connected to an Arduino Mega 2560 R3 microcontroller board using a jumper wire to read and process data prior to transmission to the server or computer (refer to Fig. 1(b) and (c)). The casing of the MPFI sensor was made using a 3D printer to protect and prevent soil particles or dust from disrupting data collection and transmission to the server. Fig. 1(d) displays the casing design with width, length and height of 2.4 cm x 2.8 cm x 1.4 cm, respectively. In this study, only two prototype sensors were developed to prove the concept of the idea.

Fig. 1(e) illustrates the prototype of the MPFI sensor used in the study. The slope movement detection sensor concept is illustrated in Fig. 1(f), where a series of MPFI is aligned vertically underground at various depths to detect and display a 3D slope movement profile. MATLAB software was employed for programming, calibration, data acquisition, and graph plotting, the description of which can be referred to in the previous author's publication [15].

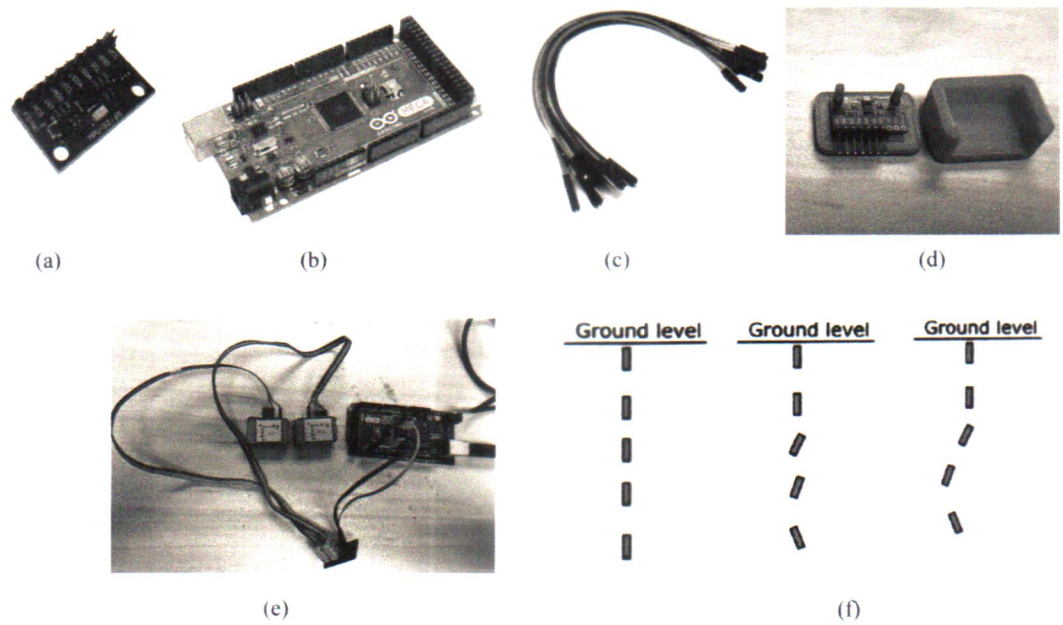

FIGURE. 1. Development of MPFI sensor (a) MPU-9250 (b) Arduino Mega 2560 R3 (c) wire (d) MPFI casing production (e) two sets of MPFI sensors connected to Arduino Mega (f) concept of slope movement detection using MPFI sensors

Experimental setup

In order to assess the effectiveness of MPFI, a small-scale slope model was constructed in an acrylic box with dimensions of 500 mm, 1,500 mm and 1,000 mm in wide, long and high, respectively, as portrayed in Fig. 2(a). An adhesive grid box sticker with a size of 10 mm x 10 mm was affixed on the side of the acrylic box to facilitate the observation of the slope movement. The silica sand was compacted manually. In particular, black and orange ink color was used to mark the soil and acrylic wall for their initial position. The marker facilitates the observation of soil slope movement and deformation measurement. The dimensions of the constructed silica sand slope model encased in the acrylic box are 500 mm wide, 1,300 mm long and 800 mm wide, forming a slope inclination angle of approximately 34° (refer Fig. 2(b)).

Two units of MPFI sensors were installed vertically underground while the Arduino Mega board was placed above the slope surface (refer to Fig. 2(c)). Both Sensor 1 and Sensor 2 were placed at depths of 3 cm and 6 cm, respectively, as displayed in Fig. 2(d). The depth was selected based on a series of trials conducted in the laboratory to determine the appropriate location to install the sensors. The mode of slope failure exhibited by silica sand material is sliding failure, where the failure plane typically extends at a shallow depth. Therefore, the MPFI sensors were embedded within the sliding plane to obtain significant movement during failure for data collection. The sliding movement would not be significant if the MPFI sensors were embedded at deeper depths.

In this study, an incremental surcharge load was applied on the top of the slope to induce slope failure. Each load weighing 8 kg is placed at an interval time of 60 seconds and then converted into uniform stress (refer to Fig. 2(e)). Fig. 2(f) illustrates the final setup of the soil slope model prior to the experiment test. The experiment was repeated for three sets, namely Experiment 1, Experiment 2 and Experiment 3, to observe the mean threshold value for slope movement. A digital clock was utilized during the experiment to determine the duration of slope failure when incremental surcharge loads were applied.

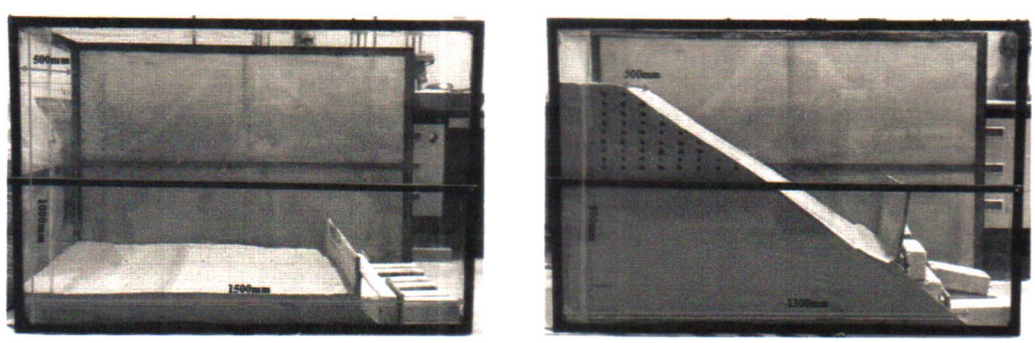

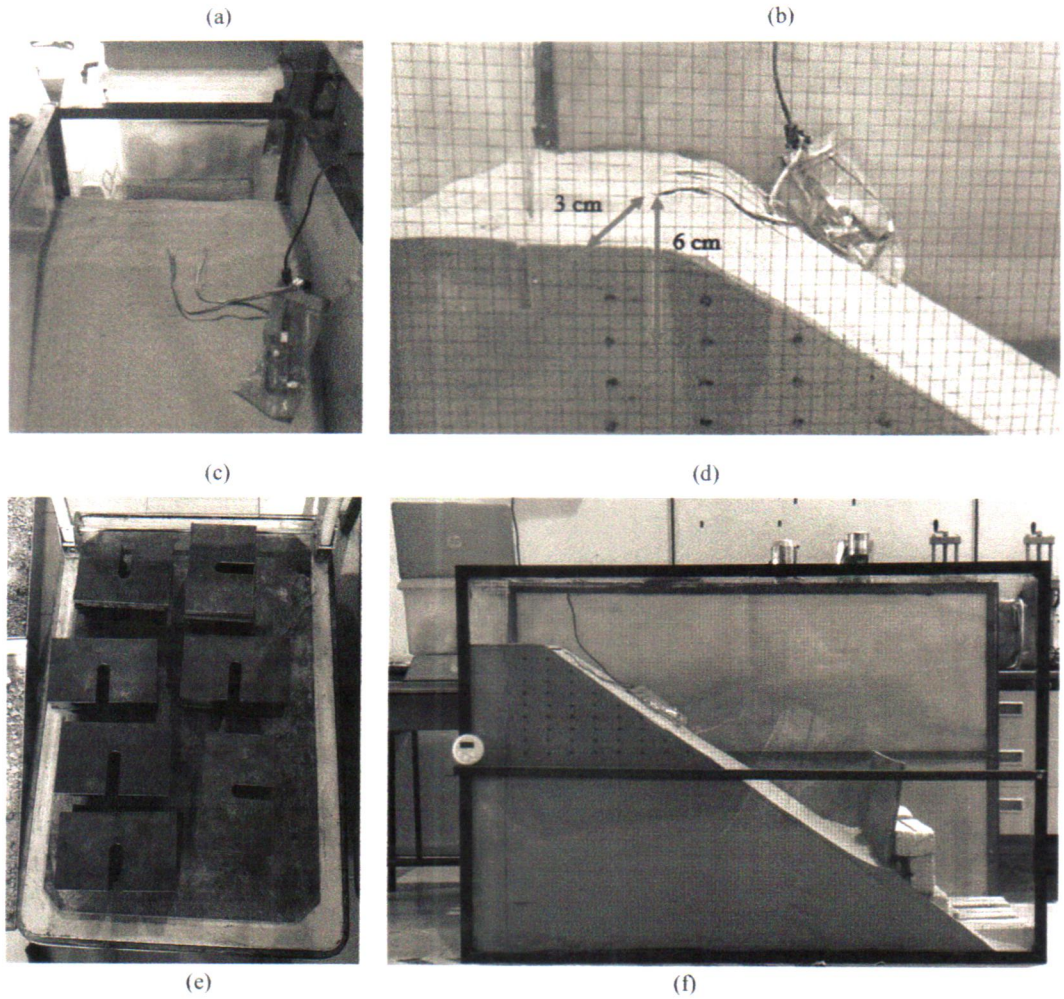

FIGURE. 2. Experimental test setup (a) dimensions of acrylic box (b) dimensions of small-scale slope model made of silica sand (c) installation of Sensors 1, Sensor 2 and microcontroller in the experiment (d) position of MPFI sensors (e) 8 kg dead load weight were used to induce slope failure (f) final setup prior to experiment test

RESULTS AND DISCUSSION

Soil properties determination

This study utilizes uniformly graded dry silica sand to construct the slope model. The soil properties were determined by a series of laboratory tests, which included sieve analysis, soil compaction, and the Consolidated-Drained (CD) triaxial compression test. Table 1 summarizes the properties of the silica sand [16,17]. The value of Cu and Cc close to 1 indicates that the sand is very uniformly graded and not perfectly sorted. Meanwhile, the E_{oed}^{ref} value indicates that the silica sand is resistant to compression when subjected to vertical loading. E_{ur}^{ref} represents the secant modulus of the soil, which defines its stress-strain behavior in triaxial loading conditions. It is derived from the hyperbolic stress-strain relationship and describes the stiffness of the soil before failure (i.e. before peak strength is reached). Notably, a value of 36798 kN/m² (~36.8 MPa) indicates the silica sand's resistance to deformation under deviatoric stress. The soil properties will be used in PLAXIS software to predict the deformation of silica sand slope using the Hardening Soil Model (HSM).

TABLE 1. Summary of silica sand properties

Soil Properties	Result	Unit
Type of soil	Well graded sand	0% gravel, 99.2% sand, 0.8% silt
Uniformity coefficient (Cu)	1.04	
Curvature coefficient (Cc)	0.9	
Optimum moisture content	16.7	%
Dry density	15.33	kN/m^3
$E50^{ref}$	36798	kN/m^2
E_{oed}^{ref}	29438	kN/m^2
E_{ur}^{ref}	110394	kN/m^2
c	8	kN/m^2
φ	40	°
ψ	0.7	°

Experimental Test

The output signal from the MPFI sensor devices needs to be interpreted to provide information relevant to detecting the movement of the slope prior to failure and determining the threshold value in terms of acceleration. In addition, an incremental surcharge load was applied on the top of the slope to induce slope failure, and simultaneously, the MPFI recorded the acceleration readings.

Fig. 3(a) depicts the acceleration-time history graph recorded by Sensor 1 and Sensor 2 in Experiment 1. The blue, red and yellow lines represent the acceleration data in the x, y, and z-axis, respectively. The MPFI sensor device successfully records the slope movement through acceleration readings until the test stops at 7.18 minutes (430 seconds) due to a loss in the signal by the failure. Note that the acceleration in the z and x-axis demonstrates dominant movement compared to the y-axis. Two significant peak accelerations are noted in the graph prior to failure, indicating slope movement during the application of surcharge load. The peak values of the alert and triggering state are 0.02 m/s^2 and 0.1 m/s^2 for both the z and x directions. Additionally, the peak of alert and triggering state for the y-axis is relatively lower, approximately 0.01 m/s^2, indicating that slope movement is less dominant in the y direction than in the z and x directions. Figs. 3(b) and (c) present the final position of both Sensor 1 and Sensor 2 in Experiment 1 in a 3D graphic.

Fig. 4 and Fig. 5 display the acceleration-time history graph for Experiment 2 and Experiment 3, respectively. The MPFI sensor continues to take the slope movement readings until the test stops at 7.05 minutes (423 seconds) for both experiments. Similarly, the peak value of the alert is slightly lower than 0.02 m/s^2, and the triggering state is higher than 0.1 m/s^2 for both z and x directions. The results are consistent for Experiment 2 and Experiment 3.

Table 2 summarizes the threshold values for slope failure categories based on the acceleration value of the x, y, and z axes. The steady condition is defined when the acceleration of the slope movement is 0 m/s^2, while the triggering zone is when the acceleration of z, x, and y acceleration exceeds 0.1, 0.1, and 0.01 m/s^2, respectively. The results suggested that acceleration in the z and x-axis is more prevalent than in the y-axis.

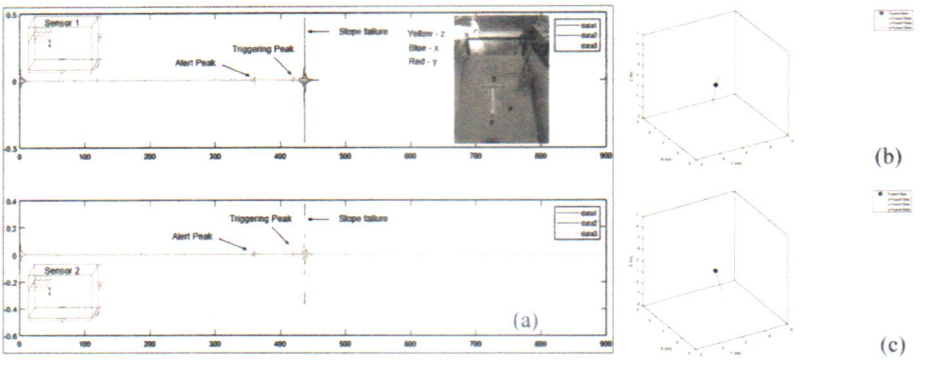

FIGURE. 3. Results of Experiment 1 (a) acceleration-time history graph (b) Final position of Sensor 1 in 3D graphics (c) Final position of Sensor 2 in 3D graphics

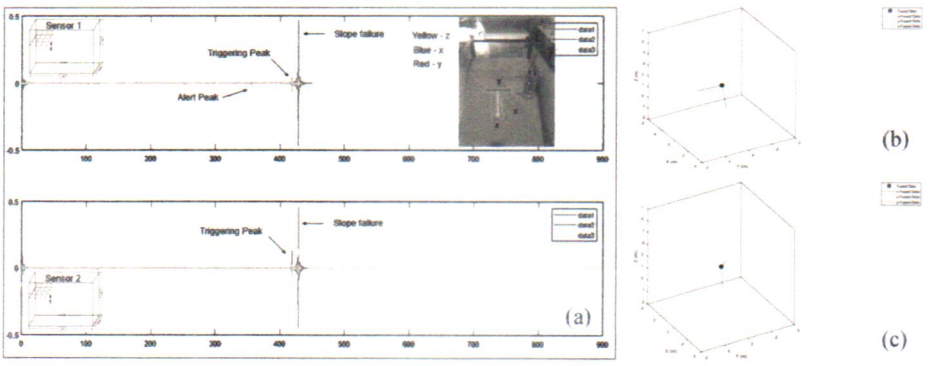

FIGURE. 4. Results of Experiment 2 (a) acceleration-time history graph (b) Final position of Sensor 1 in 3D graphics (c) Final position of Sensor 2 in 3D graphics

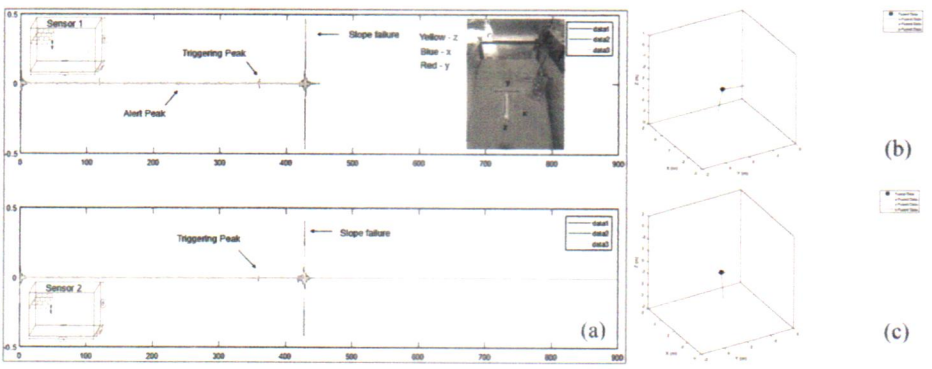

FIGURE. 5. Results of Experiment 3 (a) acceleration-time history graph (b) Final position of Sensor 1 in 3D graphics (c) Final position of Sensor 2 in 3D graphics

TABLE 2. The categories of acceleration states and the threshold value for silica sand slope

Axis	Steady (m/s^2)	Alert (m/s^2)	Triggering (m/s^2)
Z-Acceleration	0	0.02	> 0.1
X-Acceleration	0	0.02	> 0.1
Y-Acceleration	0	0.01	> 0.01

CONCLUSION

In this study, a slope movement detection sensor, the MPFI, was developed to detect the movement of the slope prior to failure and determine its threshold value in terms of acceleration through a small-scale slope model. The soil slope model was subjected to an incremental surcharge load of 6.4 kN/m^2 to initiate the movement of the slope. Accordingly, three sets of experiments were conducted in the laboratory where the MPFI sensors were placed in the slope model. The results obtained from the MPFI sensor offer the threshold values of slope failure based on x, y and z-axis acceleration. In particular, the alert values for z-acceleration and x-acceleration were 0.02 m/s^2 and 0.01 m/s^2 for y-acceleration. Meanwhile, the triggering conditions for slope failure were when the values of z-acceleration and x-acceleration exceeded 0.1 m/s^2 and 0.01 m/s^2 for y-acceleration. In essence, the results revealed that acceleration in the z and x-axis is more prevalent than in the y-axis. Nevertheless, the MPFI will be further developed for long-term monitoring with the application of the Internet-of-Thing (IoT) and early warning system.

ACKNOWLEDGMENTS

The authors wish to thank the Ministry of Higher Education (MOHE) and National Defence University of Malaysia (UPNM) for funding and supporting this project under the grant, with project code PRGS/1/2024/TK06/UPNM/02/1.

REFERENCES

1. G. Shanmugam, and Y. Wang, "The landslide problem," Journal of Palaeogeography **4**(2), 109–166 (2015).
2. S.T. McColl, "Chapter 2 - Landslide causes and triggers," in *Landslide Hazards, Risks, and Disasters (Second Edition)*, edited by T. Davies, N. Rosser, and J.F. Shroder, Second Edi, (Elsevier, 2022), pp. 13–41.
3. A. Zaki, H.K. Chai, H.A. Razak, and T. Shiotani, "Monitoring and evaluating the stability of soil slopes: A review on various available methods and feasibility of acoustic emission technique," Comptes Rendus - Geoscience **346**(9–10), 223–232 (2014).
4. M. Mukhlisin, S.J. Matlan, M.J. Ahlan, and M.R. Taha, "Analysis of Rainfall Effect to Slope Stability in Ulu Klang, Malaysia," J Teknol **72**(3(2015)), 15–21 (2015).
5. D. Kazmi, S. Qasim, I.S.H. Harahap, and T.H. Vu, "Analytical study of the causes of the major landslide of Bukit Antarabangsa in 2008 using fault tree analysis," Innovative Infrastructure Solutions **2**(1), (2017).
6. G. Singh, M.A.B.H. Abdul Rahman, and M.S. bin Zulkipli, "An Emergency and Mass Casualty Incident Response in the Jalan Batang Kali-Jalan Genting Highlands Malaysia Landslide 2022: A Case Report and Strategies to Improve," International Journal of Management and Human Sciences **07**(01), 33–40 (2023).
7. T. Ma, C. Li, Z. Lu, and Q. Bao, "Geomorphology Rainfall intensity – duration thresholds for the initiation of landslides in Zhejiang Province, China," Geomorphology **245**, 193–206 (2015).
8. R.K. Dahal, and S. Hasegawa, "Representative rainfall thresholds for landslides in the Nepal Himalaya," Geomorphology **100**(August 1998), 429–443 (2008).
9. M. Bordoni, C. Meisina, R. Valentino, N. Lu, M. Bittelli, and S. Chersich, "Hydrological factors affecting rainfall-induced shallow landslides: From the field monitoring to a simplified slope stability analysis," Eng Geol **193**, 19–37 (2015).
10. G. Urciuoli, M. Pirone, L. Comegna, and L. Picarelli, "Long-term investigations on the pore pressure regime in saturated and unsaturated sloping soils," Eng Geol **212**, 98–119 (2016).
11. R. Sheikh, Y. Nakata, M. Shitano, and M. Kaneko, "Rainfall-induced unstable slope monitoring and early warning through tilt sensors," Soils and Foundations **61**(4), 1033–1053 (2021).

12. W.H.T. Fung, R.J. Kinsil, S. Jamaludin, and S. Krishnan, "Early warning and real-time slope monitoring systems in west and east Malaysia," in *Landslide Science for a Safer Geoenvironment: Volume 2: Methods of Landslide Studies*, (2014).
13. G. Konak, A.H. Onur, D. Karakus, H. Köse, Y. Koca, and H. Yenice, "Slope stability analysis and slide monitoring by inclinometer readings: Part 2," Mining Technology **113**(3), 171–180 (2004).
14. S. Sharma, R. Kumar, and Nandakishore, "Landslide Detection Using DInSAR Technique: A Case Study," Advances in Natural and Technological Hazards Research **52**(May), 479–491 (2024).
15. A.S.A. Ishak, J. Jelani, S.M.F.S.M. Dardin, Z.A. Rashid, and Z. Suif, "Concept Development of Inclinometer for Real-Time Data Collection in Slope Movement Detection," Journal of Engineering Science and Technology **18**(1), 132–144 (2023).
16. A.S. Ahmad Ishak, J. Jelani, S.Y. Wong, Z. Suif, and A.L.A. Mazuki, "Experimental and Numerical Study on the Behaviour of Silica Sand Slope Model," J Teknol **86:1**(2024), 165–173 (2024).
17. A.S. Ahmad Ishak, J. Jelani, S.Y. Wong, Z. Suif, and A.L. Ahmad Mazuki, "Stability Analysis of a Silica Sand Slope Model Subjected To Surcharge Load Using LEM and FEM Methods," International Journal of GEOMATE **27**(121), 128–135 (2024).